THE JOURNAL OF BIOLOGICAL CHEMISTRY VOL. 290, NO. 28, pp. 17390–17400, July 10, 2015
© 2015 by The American Society for Biochemistry and Molecular Biology, Inc. Published in the U.S.A.

Human CLC-K Channels Require Palmitoylation of Their Accessory Subunit Barttin to Be Functional*

Received for publication, December 12, 2014, and in revised form, April 30, 2015 Published, JBC Papers in Press, May 26, 2015, DOI 10.1074/jbc.M114.631705

Kim Vanessa Steinke[‡1], Nataliya Gorinski[‡1], Daniel Wojciechowski[‡§], Vladimir Todorov[¶], Daria Guseva[‡], Evgeni Ponimaskin[‡], Christoph Fahlke[§2], and Martin Fischer[‡3]

From the [‡]Institut für Neurophysiologie, Medizinische Hochschule Hannover, 30625 Hannover, Germany, [§]Institute of Complex Systems, Zelluläre Biophysik (ICS-4), FZ Jülich, 52428 Jülich, Germany, and [¶]Laboratory for Experimental Nephrology, Division of Nephrology, University Hospital Dresden, 01307 Dresden Germany

Background: CLC-K channels and their subunit barttin are crucial for urinary concentration and hearing.
Results: Non-palmitoylated barttin mutants reduce CLC-K current amplitudes without modifying unitary channel properties.
Conclusion: Palmitoylation of barttin switches CLC-K channels into an active state.
Significance: Palmitoylation/depalmitoylation of CLC-K/barttin channels pre-inserted in epithelial plasma membranes might regulate renal chloride absorption.

CLC-K/barttin chloride channels are essential for NaCl re-absorption in Henle's loop and for potassium secretion by the stria vascularis in the inner ear. Here, we studied the posttranslational modification of such channels by palmitoylation of their accessory subunit barttin. We found that barttin is palmitoylated *in vivo* and *in vitro* and identified two conserved cysteine residues at positions 54 and 56 as palmitoylation sites. Point mutations at these two residues reduce the macroscopic current amplitudes in cells expressing CLC-K/barttin channels proportionally to the relative reduction in palmitoylated barttin. CLC-K/barttin expression, plasma membrane insertion, and single channel properties remain unaffected, indicating that these mutations decrease the number of active channels. R8W and G47R, two naturally occurring barttin mutations identified in patients with Bartter syndrome type IV, reduce barttin palmitoylation and CLC-K/barttin channel activity. Palmitoylation of the accessory subunit barttin might thus play a role in chloride channel dysfunction in certain variants of Bartter syndrome. We did not observe pronounced alteration of barttin palmitoylation upon increased salt and water intake or water deprivation, indicating that this posttranslational modification does not contribute to long term adaptation to variable water intake. Our results identify barttin palmitoylation as a novel posttranslational modification of CLC-K/barttin chloride channels.

Barttin is the accessory subunit of CLC-K chloride channels expressed in the kidney and the inner ear (1–4). There are two types of human CLC-K channels (5): hClC-Ka, which resides in the thin ascending limb of Henle's loop and contributes to the counter-current mechanism (6), and hClC-Kb, which is necessary for secondary-active sodium chloride re-absorption in the outer medulla and cortical region of the kidney (7). hClC-Ka and hClC-Kb are also expressed in the marginal cells of the stria vascularis in the inner ear and contribute to potassium secretion into the endolymph, a process that is crucial for sensory transduction in inner hair cells (1, 8).

Barttin was identified as a product of the disease gene of Bartter syndrome type IV, a human syndrome that combines sensorineural deafness with urinary concentration deficit (9). Barttin is an integral membrane protein that modifies the function as well as the subcellular distribution of CLC-K channels. It promotes surface membrane insertion of CLC-K/barttin channels, increases protein stability, and switches human CLC-K/barttin channels into an active state (1, 10–13). Urinary concentration mechanisms have to be regulated to permit the adjustment of renal water excretion to changes in water intake. The chloride permeability in the thin and thick ascending loop of Henle is a major determinant of the cortico-medullary osmotic gradient that determines the osmolarity of the urine. Regulation of CLC-K/barttin channels might thus be involved in adjusting water excretion and intake, and one potential target for posttranslational modification is the accessory subunit barttin with its multiple functional effects on CLC-K/barttin channels. Posttranslational modification of ion channels by palmitoylation has been shown to affect channel functions such as gating and pharmacology (14–18). Moreover, palmitoylation is known to regulate subcellular trafficking of integral membrane proteins (19–22) or to increase the affinity of certain proteins to specific micro-domains such as lipid rafts within the cell membrane (19, 23–26).

Palmitoylation is a covalent attachment of long chain fatty acids (*i.e.* palmitate) to a cysteine residue(s) within the protein via a labile thioester linkage (19, 27). Here, we study palmitoylation of barttin as a potential regulatory pathway and charac-

* This work was supported by Deutsche Forschungsgemeinschaft Grants FA301/10 (to Ch. F.) and PO732 (to E. P.) and by Cluster of Excellence REBIRTH. (A preliminary account was presented at the 91st Annual Meeting of the Deutsche Physiologische Gesellschaft (DPG), March 22–25, 2012, Dresden, Germany (Steinke, K. V., Gorinski, N., Wojciechowski, D., Ponimaskin, E., Fischer, M., and Fahlke, Ch. (2012) *Acta Physiol.* **204,** Suppl. 689 (Abstr. P262)). The authors declare that they have no conflicts of interest with the contents of this article.
[1] Both authors contributed equally to this work.
[2] To whom correspondence may be addressed: Institute of Complex Systems, Zelluläre Biophysik (ICS-4), FZ Jülich, Leo-Brandt-Str., 52428 Jülich, Germany. Tel.: 49-2461-613016; E-mail: c.fahlke@fz-juelich.de.
[3] To whom correspondence may be addressed: Institut für Neurophysiologie, Medizinische Hochschule Hannover, Carl-Neuberg-Str. 1, 30625 Hannover, Germany. Tel.: 49-511-532-2773; Fax.: 49-511-532-2776; E-mail: fischer.martin@mh-hannover.de.

terize the effects of barttin palmitoylation on CLC-K/barttin channel function. Our data show that palmitoylation of barttin is necessary for activation of plasma membrane-inserted CLC-K/barttin channels.

Experimental Procedures

Heterologous Expression and Mutagenesis—We used heterologous expression in two different cell lines, MDCK II[4] and HEK293T cells, to study intracellular trafficking and function of hClC-Ka/barttin and hClC-Kb/barttin (12, 13, 28, 29). CLC-K/barttin function and subcellular distribution are comparable in both systems (12, 30), and both systems are well suited for biochemical analyses. However, HEK293T cells robustly express CLC-K/barttin and are thus perfect for the functional characterization of mutations that decrease macroscopic current amplitudes. MDCK II cells are an established model system to study targeting in epithelial cells. HEK293T and MDCK II cells were transfected with plasmids DNA encoding hClC-Ka, hClC-Kb, or human barttin (12, 28) using the calcium phosphate precipitation method (31) or Lipofectamine 2000 (Invitrogen). In some of the experiments CFP or YFP fusion proteins of CLC-K channels and barttin were transfected (28). Mutant barttins were constructed using the QuikChange site-directed mutagenesis kit (Stratagene, La Jolla, CA). For all constructs, PCR-amplified sequences were verified by direct sequencing, and two independent mutant clones were used for expression studies.

Analysis of Barttin Palmitoylation—Palmitoylation of heterologously expressed barttin was investigated after transient transfection of HEK293T cells with pcDNA3.1 plasmid DNA encoding for human barttin-mCFP fusion protein. For experiments using radioactive palmitate, transfected HEK293T cells were labeled with [^{3}H]palmitate (300 μCi/ml, 30–60 Ci/mmol) for 2 h 1 day after transfection. Barttin-mCFP was immunoprecipitated with anti-GFP antibodies (rabbit polyclonal to GFP; GeneTex), and radiolabeled polypeptides were analyzed by sodium dodecyl sulfate-polyacrylamide gel electrophoresis (SDS-PAGE) on 10% acrylamide gels under non-reducing conditions followed by fluorography.

A modified protocol for proteomic acyl-biotinyl exchange (ABE) (32) was used to analyze palmitoylation of barttin in native tissue. After homogenization of mouse kidneys, free thiol groups were blocked by treatment with 10 mM *N*-ethylmaleimide. Thioester-linked palmitoyl moieties were then cleaved by treatment with 0.5 M hydroxylamine (plus NH_2OH) followed by labeling of the free thiol groups with 0.75 mM thiol-reactive biotinylation reagent (HPDP-biotin). Biotinylated proteins were purified by streptavidin-agarose affinity chromatography, subjected to SDS-PAGE on 10% acrylamide gels, and identified by Western blot with anti-barttin antibody (sc-49611; Santa Cruz Biotechnology). Samples without hydroxylamine treatment (minus NH_2OH) served to identify unspecific binding of biotin.

To analyze the palmitoylation of heterologously expressed barttin-mCFP, cells were subjected to ABE followed by immunoprecipitation of barttin-mCFP with anti-GFP-Sepharose and Western blot with anti-biotin-specific antibody allowing for specific detection of palmitoylated protein. Samples without NH_2OH were used as the negative control. Barttin palmitoylation levels were defined by densitometric analysis of barttin protein bands after ("plus NH_2OH") or without hydroxylamine treatment ("minus NH_2OH" bands). After normalization to the corresponding expression levels, as defined by the Western blot of total lysates, values from the samples without NH_2OH treatment were subtracted from corresponding values obtained in samples treated with NH_2OH to correct for unspecific signals. For every barttin mutant, palmitoylation level was given as relative value in comparison to WT barttin, which was set to 100%.

To investigate the influence of dehydration on barttin palmitoylation, mice had either free access to tap water (normal condition) or were deprived of water for 24 h (dehydrated condition) before kidney extirpation. We further studied barttin palmitoylation under a high salt diet for 7 days, where animals had free access to water and food that was balanced in all respects except for high sodium chloride content (4% NaCl; Ssniff, Soest, Germany) (33). Control animals were fed with a standard diet (0.3% NaCl). Animal care and experimentation were approved by the local animal ethics committee and carried out in accordance with National Institutes of Health Principles and Guidelines for the Care and Use of Laboratory Animals.

Electrophysiology and Data Analysis—For electrophysiological experiments, HEK293T cells were co-transfected with 2 μg of pcDNA3.1 plasmid DNA encoding human barttin-mCFP and 2 μg of pSVL plasmid DNA encoding hClC-Ka or hClC-Kb. Only fluorescent cells were used for electrophysiological recordings. Standard whole-cell patch clamp recordings were performed typically 1 day after transfection using an Axopatch 200B amplifier (Molecular Devices, Sunnyvale, CA). Pipettes were pulled from borosilicate glass (Harvard Apparatus, Holliston, MA) with resistances of 1.0–2.0 megaohms. For noise analyses, pipettes were covered with dental wax to reduce their capacitance. Agar bridges were used to connect the amplifier and the bath solution. 90–95% of the series resistance was compensated by an analog procedure. Cells were clamped to 0 mV for 1–7 s between test sweeps. The standard extracellular solution contained 140 mM NaCl, 4 mM KCl, 2 mM $CaCl_2$, 0.5–1 mM $MgCl_2$, 5 mM HEPES, pH 7.4. The standard intracellular solution contained 120 mM NaCl, 2 mM $MgCl_2$, 5 mM EGTA, 10 mM HEPES, pH 7.4. Patch clamp recordings were performed as described using standard intra- and extracellular solutions at least 1 day after transfection.

Data were analyzed using a combination of Clampfit (Axon Instruments, Union City, CA) and SigmaPlot (Systat Software Inc., San Jose, CA) programs. To determine the unitary conductances as well as absolute open probabilities of hClC-Ka/barttin channels, stationary noise analysis was performed as described previously (29, 34). Currents were filtered at 10 kHz and digitized with a sampling rate of 50 kHz. Current variances were corrected for the background variance that was measured at the reversal potential ($Vr = -5$ mV).

Ion channels generate a Lorentzian type of noise (σ^2) that depends on the number of channels (N), the unitary current amplitude (i), and the absolute open probability (p),

[4] The abbreviations used are: MDCK Madin-Darby canine kidney; CFP, cyan fluorescent protein; mCFP, monomeric CFP; ABE, acyl-biotinyl exchange.

$$\sigma^2 = Ni^2p(1 - p) \quad \text{(Eq. 1)}$$

Implementing the macroscopic current amplitude (I, with $I = Nip$), Equation 1 can be modified to

$$\sigma^2 = iI - \frac{I^2}{N} \quad \text{(Eq. 2)}$$

or

$$\frac{\sigma^2}{I} = i - \frac{I}{N} \quad \text{(Eq. 3)}$$

In the case of non-stationary noise analysis at a fixed potential, fitting parabolic functions to variance *versus* current plots (35) or linear functions to σ^2/I *versus* current plots (36) provides unitary current amplitudes (i) and the number of active channels (N). The very fast deactivation of hClC-Ka/barttin channels at negative potentials (29) makes non-stationary noise analysis difficult, and we, therefore, applied a modification of steady-state noise analysis. We determined steady-state current variances and steady-state current amplitudes for various voltages and normalized the current variance by the product of the mean current amplitude (I) and the electrical driving force ($V - Vr$) and plotted this quotient *versus* the macroscopic conductance ($I/(V - Vr)$),

$$\frac{\sigma^2}{I(V - Vr)} = \frac{i}{(V - Vr)} - \frac{1}{N} \cdot \frac{I}{(V - Vr)} \quad \text{(Eq. 4)}$$

Because the unitary conductance $\gamma = i/(V - Vr)$ is constant for hClC-Ka/barttin channels (29, 34), Equation 4 simplifies to

$$\frac{\sigma^2}{I(V - Vr)} = \gamma - \frac{1}{N} \cdot \frac{I}{(V - Vr)} \quad \text{(Eq. 5)}$$

In such a plot the negative inverse slope of the linear regression reveals the number of active channels in the cell membrane, and the y axis intercept represents the unitary channel conductance (γ).

Biochemical Analysis of Protein Expression and Surface Membrane Insertion—Expression of barttin and CLC-K channels was analyzed using transiently transfected MDCK II cells. Cells were lysed by incubation in 1% Triton X-100 in the presence of protease inhibitors (Sigma). Cleared lysates were denatured for 15 min at room temperature in SDS sample buffer containing 100 mM dithiothreitol and electrophoresed in parallel with fluorescence mass markers (Dual Color; Bio-Rad) on 12% SDS-polyacrylamide gels. mCFP-tagged barttin and YFP-tagged hClC-Ka were visualized by scanning the wet PAGE gels with a fluorescence scanner (Typhoon; GE Healthcare). Fluorescence intensities of individual bands were quantified with the ImageQuant software (GE Healthcare).

For analysis of cell surface expression of CLC-K/barttin channels, MDCK II cells were incubated for 40 min with 0.25 mg of biotin (EZ link sulfo-NHS-SS-biotin; Pierce) before cell lysis (28, 37). Biotinylated proteins were purified using NeutrAvidin affinity chromatography (Pierce) and separated by electrophoresis on 12% SDS-polyacrylamide gels. Fluorescence scans of the gels revealed the relative amounts of membrane-inserted YFP-hClC-Ka channels in the presence of WT and mutant barttin-mCFP. Contamination of purified protein fractions by intracellular proteins was checked by Western blots of the gels with mouse anti-GAPDH (GeneTex Inc.). Results were taken only from experiments without GAPDH detection.

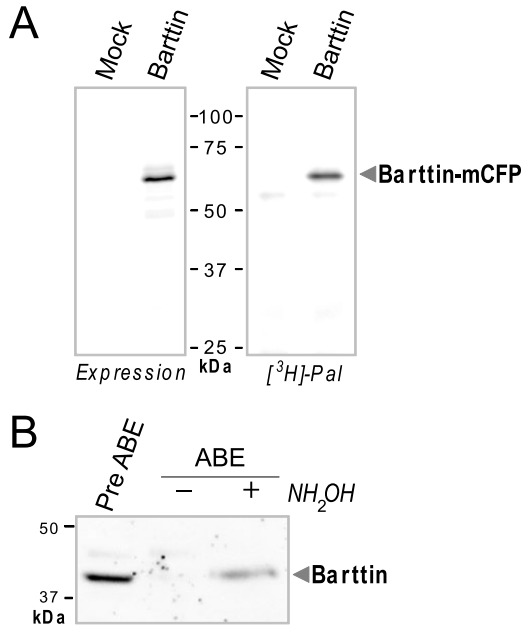

FIGURE 1. **Barttin is palmitoylated in heterologous expression systems and in native cells.** *A*, HEK293T cells expressing barttin-mCFP were labeled with [^{3}H]palmitate and subjected to immunoprecipitation with anti-GFP antibodies followed by SDS-PAGE and fluorography after 7 days exposure (*right panel*). Expression of barttin-mCFP was documented by fluorescence detection (*left panel*). Representative results from one of two independent experiments are shown. *B*, representative ABE analysis of barttin palmitoylation in mouse kidneys at postnatal day 30 followed by SDS-PAGE and Western blot. Hydroxylamine (plus NH_2OH) cleaves the thioester bond between a cysteine residue and palmitate and allows incorporation of biotinylated analog of palmitate to the newly available thiol group that can be detected by Western blot. The samples without hydroxylamine (minus NH_2OH) function as a negative control for specific palmitoyl-biotinylation. Shown is a representative blot from three independent experiments.

Confocal Microscopy—Live cell confocal imaging was carried out with transiently transfected MDCK II cells grown on special confocal tissue culture-treated dishes (Ibidi, Martinsried, Germany). Confocal images were obtained after 2–3 days of expression of fluorescent barttin-mCFP and YFP-hClC-Ka using a Leica DM IRB confocal microscope with a TCS SP2 AOBS scan head (Leica Microsystems, Wetzlar, Germany).

Data are shown as the means ± S.E. Unpaired Student's t test was performed to prove statistical significance of differences in mean values.

Results

Barttin Is Palmitoylated at Cysteine Residues Cys-54 and Cys-56—To test whether human barttin is palmitoylated we metabolically labeled recombinant mCFP-tagged barttin with [^{3}H]palmitate in HEK293T cells. After lysis and immunoprecipitation with polyclonal antibodies against GFP, we resolved a single [^{3}H]palmitate-bound protein band after SDS-PAGE and fluorography (Fig. 1*A*). This protein co-migrated with barttin-mCFP, as detected by fluorescence imaging, demonstrating that barttin is palmitoylated in heterologous expression systems.

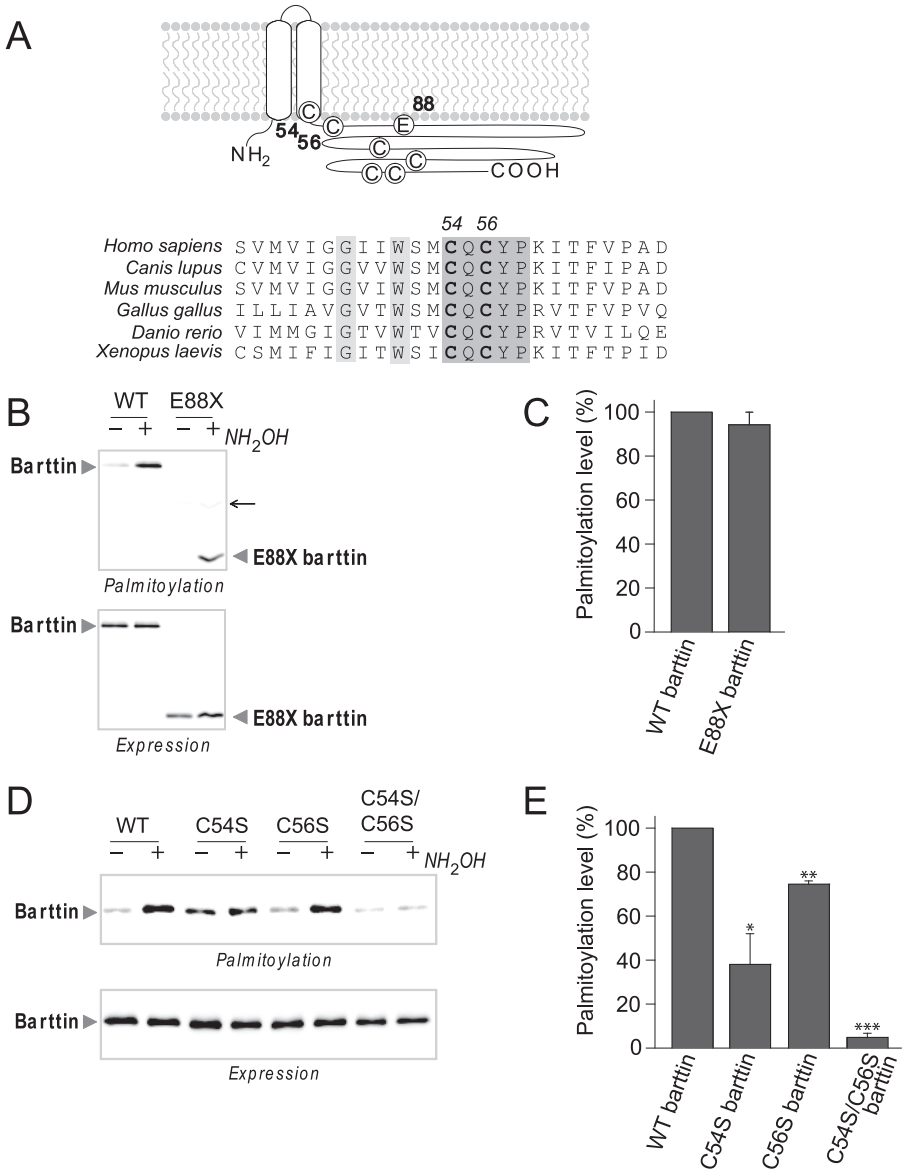

FIGURE 2. **Identification of two palmitoylation sites in barttin.** *A*, putative topology of barttin (*upper panel*) and amino acid sequence of barttin surrounding highly conserved cysteine residues Cys-54 and Cys-56 for different species (*lower panel*). *B–E*, representative images of the ABE assay and quantitative analysis of palmitoylation for WT and E88X barttin (*B* and *C*) and for WT, C54S, C56S, and C54S/C56S (*D* and *E*). Palmitoylation levels were calculated by comparison of corresponding samples with and without NH_2OH (negative control) treatment after normalization to the expression level. Data represent the means ± S.E. from three independent experiments. *, $p < 0.05$; **, $p < 0.01$; ***, $p < 0.001$). We observed a low intensity unspecific band with a molecular mass of ~50 kDa (marked by an *arrow* in *B*) in all experiments with WT and mutant barttin-mCFP.

We then used a modified proteomic ABE technique (32) to analyze barttin palmitoylation in native renal cells. This technique does not require metabolic labeling of cells or tissues and, therefore, permits identification of protein palmitoylation in their native surrounding. The ABE technique is based on the cleavage of thioester linkages between cysteines and palmitates by hydroxylamine (NH_2OH). Cleavage of the thioester link allows the specific incorporation of a biotinylated analog of palmitate (HPDP-biotin) to the newly available thiol group and permits detecting biotinylated palmitate analogs by Western blotting. Using this approach we could demonstrate *in vivo* posttranslational palmitoylation of endogenous barttin in mouse kidneys (Fig. 1*B*).

The predicted barttin topology consists of two transmembrane helices, a short intracellular N terminus and a long intracellular C terminus (1, 9) (Fig. 2*A*). There are six cysteine residues that are all located within the C terminus. To identify potential palmitoylation sites, we took advantage of a recently characterized disease-associated truncation mutation of barttin, E88X (28), that removes four of the six cysteines. Upon heterologous expression in HEK293T cells, no differences in palmitoylation levels of WT and E88X barttin were observed (Fig. 2, *B* and *C*). This finding demonstrates that the four cysteines C terminal to Glu-88 are not used as palmitoylation sites.

The remaining two endogenous cysteines, Cys-54 and Cys-56, are localized close to the second transmembrane helix and are highly conserved (Fig. 2*A*). We next individually or jointly mutated these residues, Cys-54 and Cys-56, to serines in the non-truncated barttin-mCFP background and tested the consequences on barttin palmitoylation using ABE. Individual sub-

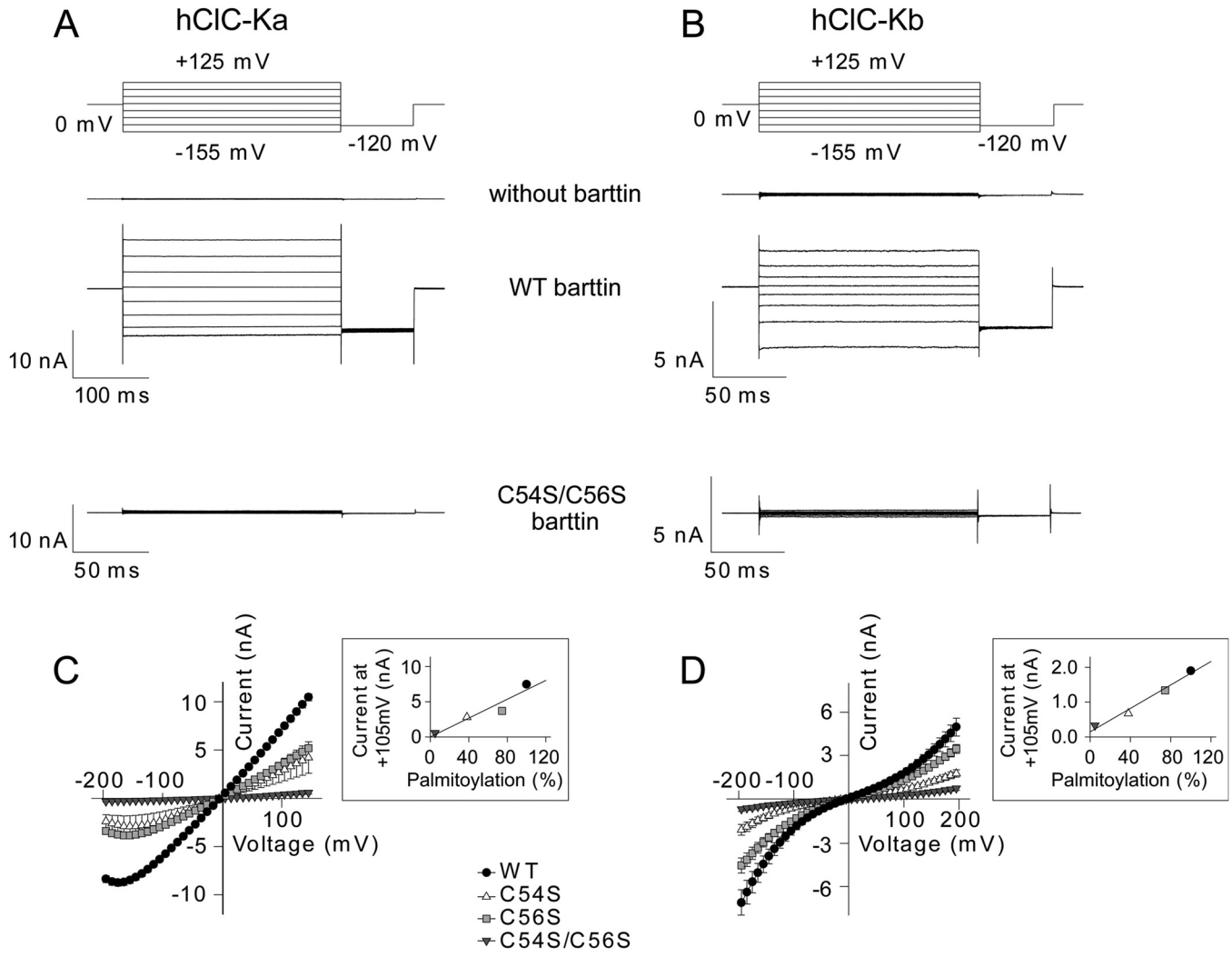

FIGURE 3. **Mutations that reduce barttin palmitoylation decrease macroscopic CLC-K/barttin currents.** *A* and *B*, voltage protocol and representative current recordings from HEK293T cells expressing hClC-Ka (*A*) or hClC-Kb (*B*) channels in the presence of WT barttin or mutant C54S/C56S barttin. *C* and *D*, voltage dependence of mean current amplitudes obtained from HEK293T cells expressing hClC-Ka (*C*) or hClC-Kb channels (*D*) in the presence of WT barttin or mutant barttin (*C*: WT, $n = 26$; C54S, $n = 11$; C56S, $n = 21$; C54S/C56S, $n = 14$; D: WT, $n = 13$; C54S, $n = 7$; C56S, $n = 7$; C54S/C56S, $n = 11$). *Insets* display plots of current amplitudes at +105 mV *versus* palmitoylation level for WT and mutant barttin.

stitutions of Cys-54 or Cys-56 resulted in significant reduction of barttin palmitoylation to 38.0 ± 13.9% or 74.5 ± 1.4% ($n = 3$), respectively. When both cysteines were mutated simultaneously, barttin palmitoylation was completely abolished (Fig. 2, *D* and *E*). We conclude that both Cys-54 and Cys-56 represent palmitoylation sites of human barttin.

Barttin Palmitoylation Is Necessary for CLC-K/barttin Currents—Fig. 3 shows representative whole-cell current recordings of human hClC-Ka and hClC-Kb channels in the absence of barttin or co-expressed with WT or non-palmitoylated C54S/C56S barttin in HEK293T cells. For these recordings the membrane potential was held at 0 mV, and voltage steps between −155 mV and +125 mV were applied, each followed by a fixed step to −120 mV. In agreement with earlier results (1, 10, 12), expression of hClC-Ka and hClC-Kb only results in measurable chloride currents when co-expressed with barttin (Fig. 3, *A* and *B*). Currents increase instantaneously upon voltage steps in the presence of WT barttin. Whereas single point mutations at positions Cys-54 or Cys-56 reduced current amplitudes, C54S/C56S barttin abolished hCLC-K/barttin currents (Fig. 3, *C* and *D*). The voltage dependence of hCLC-K/barttin currents was not affected. A plot of palmitoylation levels of different barttin mutants and corresponding hClC-Ka/barttin and hClC-Kb/barttin current amplitudes shows a linear relationship between barttin palmitoylation and chloride current amplitudes (Fig. 3, *C* and *D*, *insets*).

Barttin Palmitoylation Does Not Modify Unitary Channel Properties of CLC-K/barttin—Reduced whole-cell currents might be caused by impaired protein translation, stability, or intracellular transport or by changes in channel function. We employed stationary noise analysis to determine unitary properties of hClC-Ka/barttin channels in the presence of WT or mutant barttin (Fig. 4*A*). Because the double mutant C54S/C56S reduced hClC-K/barttin currents to levels that are too small to be reliably evaluated, we restricted this analysis to barttin mutants with only one palmitoylation site, *i.e.* C54S or C56S barttin. Plotting the current variances σ^2, normalized by the product of the mean current amplitude I and the electrical driv-

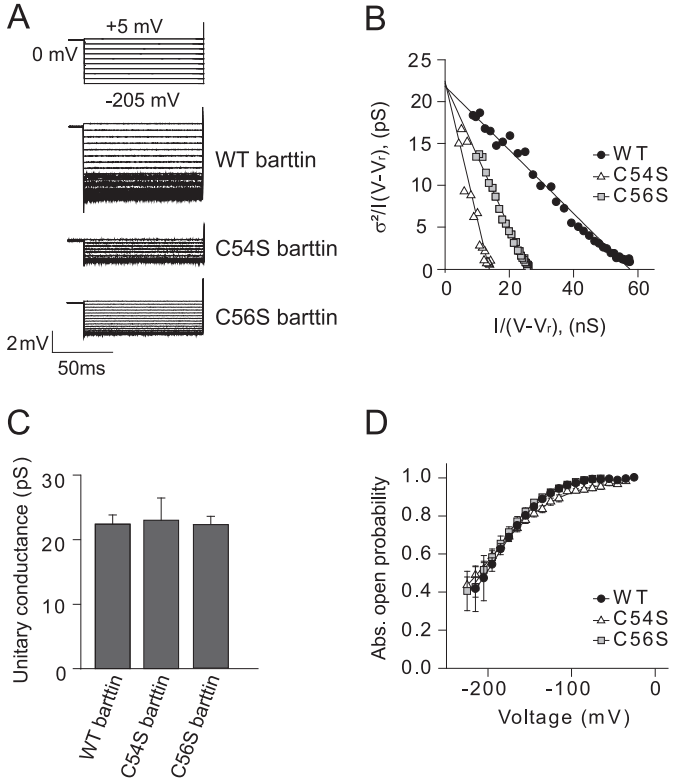

FIGURE 4. **Barttin palmitoylation does not modify unitary current amplitudes or absolute open probabilities of hClC-Ka/barttin channels.** *A*, voltage protocol for stationary noise analyses and representative current recordings of hClC-Ka co-expressed with WT or mutant barttin. *B*, plot of the variance (σ^2), normalized by the product of the mean current (*I*) and the electrical driving force ($V - Vr$), *versus* the macroscopic conductance $I/(V - Vr)$. A linear fit provides the unitary conductance as the *y* axis intercept and the number of channels as the inverse slope. *C* and *D*, unitary conductances (*C*) and absolute open probabilities (*D*) of hClC-Ka/barttin channels for WT, C54S, and C56S barttin (*C*, WT, $n = 9$; C54S, $n = 6$; C56S, $n = 8$; *D*, WT, $n = 9$; C54S, $n = 11$; C56S, $n = 8$).

ing force $V - Vr$, *versus* the macroscopic conductance $I/(V - Vr)$ displays a linear relationship (Fig. 4*B*). In such a plot the *y* axis intercept gives the unitary channel conductance, and the slope of the linear regression corresponds to the number of active channels in the plasma membrane ($N = -1$/slope) (29, 34). The unitary current conductance of hClC-Ka/barttin channels remained unaffected by the barttin mutations (Fig. 4*C*). Absolute open probabilities were calculated by dividing the macroscopic current amplitude by the number of channels and the single channel current amplitude (Fig. 4*D*). Neither absolute open probabilities nor voltage dependence of hClC-Ka activation was affected by the modified barttin subunits. We conclude that palmitoylation of barttin modifies the number of active channels in the plasma membrane but leaves CLC-K/barttin channel properties unaffected.

Barttin Palmitoylation neither Affects CLC-K Channel Biogenesis nor Intracellular Trafficking—We next tested the potential effects of barttin palmitoylation on its subcellular distribution and the trafficking of hClC-K/barttin channels. We first analyzed the intracellular distribution of barttin-mCFP by confocal microscopy, either expressed alone or together with YFP-hClC-Ka channels in MDCK II cells. WT and single-palmitoylated barttin mutants, C54S or C56S, were properly inserted into the surface membrane (Fig. 5*A*), and even the

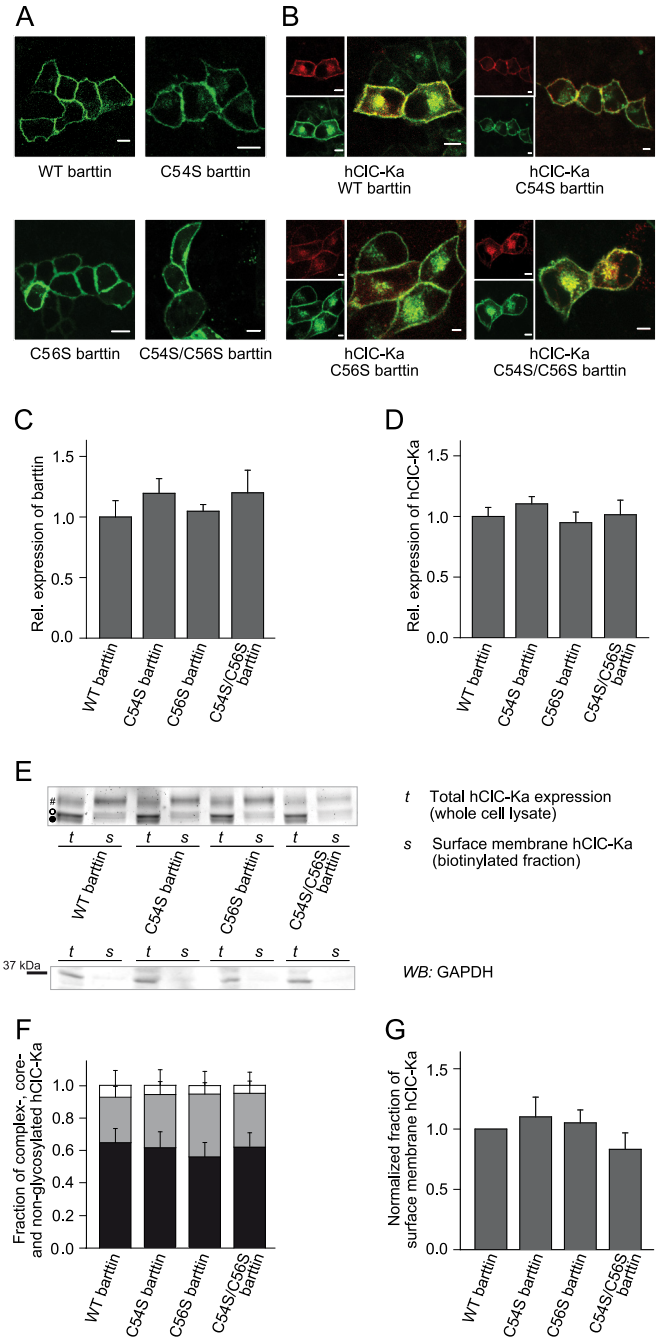

FIGURE 5. **Barttin palmitoylation does not affect the expression and subcellular distribution of hClC-Ka/barttin channels.** *A* and *B*, confocal images of MDCK II cells expressing barttin-mCFP alone (*green*) (*A*) or together with YFP-hClC-Ka (*red*) (*B*). *Scale bars* represent 10 μm. *C* and *D*, expression levels of WT or mutant barttin-mCFP (*C*) and co-expressed YFP-hClC-Ka (*D*) obtained from relative fluorescence values in SDS-PAGE gels of total cleared cell lysates. Cells were transfected with equal amounts of plasmid DNA. Data represent the means ± S.E. from at least 6 experiments in *C* and at least 12 experiments in *D*. *E*, fluorescence scan (*upper panel*) of an SDS-PAGE gel of YFP-ClC-Ka present in the total cleared lysate and the purified surface proteins when expressed together with WT or mutant barttin. Different protein bands correspond to complex-glycosylated (#) as well as core-glycosylated (○) or non-glycosylated (●) YFP-hClC-Ka. Western blot analysis of the gel using anti-GAPDH antibodies (WB, *lower panel*) validates exclusive biotinylation of surface membrane proteins. *F*, fractions of complex (*white*)-, core (*gray*)-, and non (*black*)-glycosylated YFP-hClC-Ka in whole cell lysates of HEK293T cells co-expressing WT or mutant barttin. Data are the means ± S.E. from at least six experiments. *G*, surface-biotinylated YFP-hClC-Ka quantified by YFP fluorescence and normalized to WT barttin from cells co-expressing WT or mutant barttin. Data represent the means ± S.E. from at least 10 experiments.

double mutant C54S/C56S was well expressed and clearly membrane-associated. Moreover, all mutant barttins effectively promoted trafficking of hClC-Ka channels to the plasma membrane (Fig. 5*B*).

We next compared the total expression of channel subunits in cells co-expressing hClC-Ka with WT or mutant barttin. We found that the tested mutations neither modified expression levels of barttin nor of co-expressed hClC-Ka (Fig. 5, *C* and *D*). SDS-PAGE gels display three fluorescent bands corresponding to complex-glycosylated (mature), core-glycosylated, and non-glycosylated YFP-hClC-Ka (Fig. 5*E*) (28). CLC-K channels are predominantly non- or core-glycosylated when expressed alone (28), and co-expression with barttin increases the amount of the complex-glycosylated pore-forming subunit. The relative amount of the distinct glycosylation states was similar upon co-expression with WT or mutant barttin (Fig. 5*F*). We next determined the percentage of surface membrane-inserted hClC-Ka from the fraction of proteins that was accessible to biotinylation from the extracellular side before cell lysis. The percentage of complex-glycosylated hClC-Ka was increased in the biotinylated fraction as compared with the full cell lysate. However, we also found non-glycosylated as well as core-glycosylated hClC-Ka proteins in the surface membrane (Fig. 5*E*). These results, which are closely similar to our previous results on CLC-K/barttin (28), indicate that CLC-K proteins can also insert into the plasma membrane in their non-complex-glycosylated form. These findings are in full agreement with results on other membrane proteins (38, 39). We routinely checked the surface membrane fraction for contamination with intracellular proteins by Western blots of the gels using anti-GAPDH antibodies (Fig. 5*E*, *lower panel*). There is clear antibody labeling of GAPDH in the whole cell lysate (*t*), but such a signal is absent in the biotinylated protein fraction of the surface membrane (*s*).

The fractions of surface membrane inserted channels showed slight but insignificant reduction when hClC-Ka was co-expressed with double mutant C54S/C56S barttin instead of WT barttin (Fig. 5*G*). This effect, however, was too small to explain the radical decline of current amplitudes. Palmitoylation-deficient barttin mutants reduce the amplitude of whole-cell hClC-Ka currents, whereas the subcellular trafficking and the number of channels inserted in the surface membrane were virtually unaltered. We conclude that the pronounced current reduction in cells expressing non-palmitoylated barttin results from insertion of constitutively closed hClC-Ka/barttin channels into the surface membrane. Barttin mutants with only one palmitoylation site (C54S or C56S) release some channels from their inactive state and give rise to small chloride conductance with unaltered unitary channel properties. Because stably closed channels do not influence macroscopic current variance, this conclusion is in agreement with our results from noise analysis.

Disease-associated BSND Mutations Affect Palmitoylation of Barttin—Mutations in *BSND*, the gene encoding barttin, cause Bartter syndrome type IV, an inherited disease characterized by severe impairment of urinary concentration ability and sensorineural deafness (40, 41). We recently reported that various point mutations in *BSND* result in impaired CLC-K/barttin channel activity without dramatic changes in subcellular distribution (4, 28, 29). Because of the similar effects of palmitoylation-deficient and disease-associated mutants, we reasoned that certain naturally occurring mutations might impair palmitoylation.

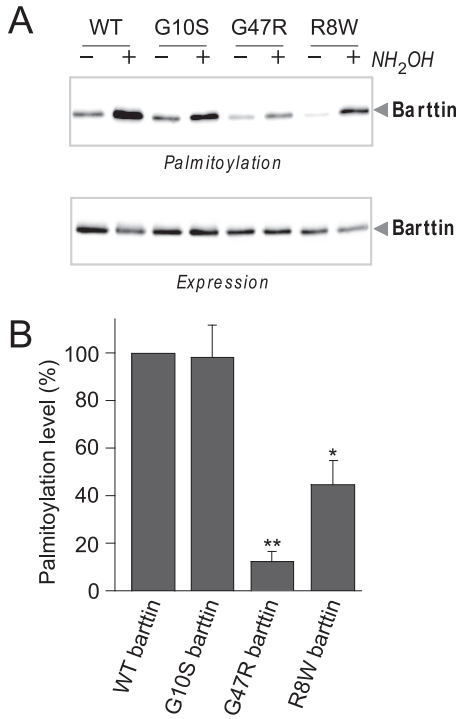

FIGURE 6. **Disease-causing mutations affect palmitoylation of barttin.** *A*, representative image from ABE palmitoylation assay followed by SDS-PAGE and Western blot for WT, G10S, G47R, and R8W barttin. *B*, relative palmitoylation levels of WT and barttin mutants. Data are given as the means ± S.E. from three independent experiments. *, $p < 0.05$; **. $p < 0.01$.

We tested three disease-associated barttin mutations (R8W, G10S, and G47R) for their possible deficiencies in palmitoylation. G47R exerted the most pronounced effect on barttin palmitoylation and reduced relative palmitoylation to 12.3 ± 3.0% ($n = 3$) of WT values. Although palmitoylation of R8W barttin was reduced to 44.6 ± 7.2% ($n = 3$), there was no effect of the G10S mutation (Fig. 6). We conclude that some, but not all disease-causing *BSND* mutations affect palmitoylation of barttin.

Changes in Barttin Palmitoylation upon Increased or Decreased Water Intake—The inner medullar osmolarity of the kidney is crucially dependent on the chloride permeability of the thin and the thick ascending limb of Henle's loop. Regulated palmitoylation (for example, under water shortage) might, therefore, stimulate urinary concentration and reduce water excretion. We thus tested the effect of water deprivation or increased water intake upon salt diet on barttin palmitoylation levels.

In experiments testing the effect of reduced water intake barttin palmitoylation was quantified in kidneys from mice deprived of water for 1 day and compared with normally hydrated control animals. Dehydration slightly increased the level of barttin palmitoylation as compared with control animals with no water restriction, whereas the expression level of barttin remained unaffected (Fig. 7, *A-C*). However, when animals were fed with high salt diet (4% NaCl for 7 days) resulting in 2-fold water intake without any change in body weight, elevated diuresis was not related to significant changes in barttin palmitoylation or expression (Fig. 7, *D–G*). We conclude that

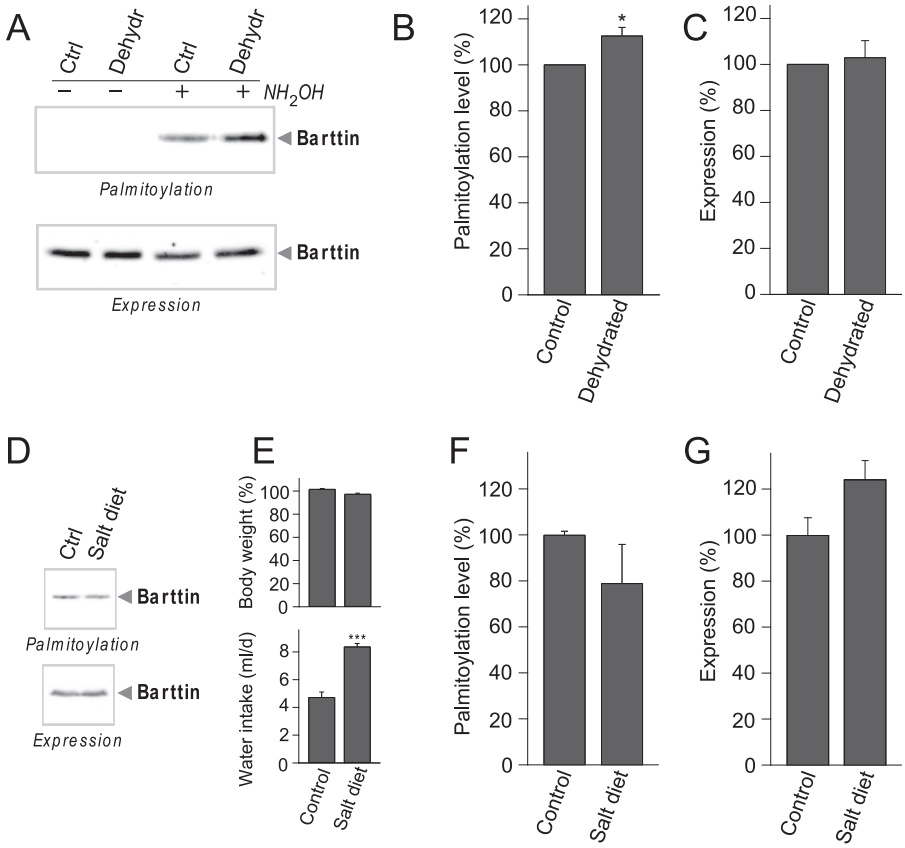

FIGURE 7. **Barttin palmitoylation is only slightly modified by the hydration status.** *A*, representative image of barttin palmitoylation in kidneys from dehydrated and control mice as assessed by ABE assays followed by SDS-PAGE and Western blot. *B* and *C*, relative palmitoylation (*B*) and expression levels (*C*) of barttin in kidneys of dehydrated and control mice. Data represent the means ± S.E. from five independent experiments. *D*, representative image from ABE assays followed by SDS-PAGE and Western blot for kidneys from mice after a high salt diet and from control mice after NH_2OH treatment. *E*, comparison of body weight and water intake of control and test mice. *F* and *G*, relative palmitoylation (*F*) and expression levels (*G*) of barttin in the kidneys of control and test mice. Data are given as the means ± S.E. from at least four independent experiments. (*, $p < 0.05$; ***, $p < 0.001$).

changes in water intake do not significantly alter palmitoylation of barttin.

Discussion

Here we demonstrate that barttin, the accessory subunit of CLC-K channels, is palmitoylated *in vivo* as well as *in vitro* (Fig. 1). Two cysteine residues, Cys-54 and Cys-56, localized at the junction between the second transmembrane helix and the cytoplasmic C terminus, represent palmitoylation sites of barttin (Fig. 2). Expression of palmitoylation-deficient barttin mutants caused a dramatic reduction of macroscopic current amplitudes (Fig. 3). The changes in current amplitudes are not due to altered subcellular trafficking or membrane insertion (Fig. 5) but rather result from impaired function of CLC-K/barttin channels in the presence of non-palmitoylated barttin. We conclude that hClC-K channels are switched into an active state by palmitoylated barttin but remain inactive with palmitoylation-deficient barttin mutants.

In the past 2-bromo-palmitate has often been used as pharmacological tool to block protein palmitoylation. Unfortunately, 2-bromo-palmitate exerts pleiotropic and unspecific effects (42) so that this compound cannot be used to test the consequences of barttin palmitoylation on CLC-K/barttin function. We, therefore, employed mutant barttins, in which either one of the two or both palmitoylation sites were removed, to test the functional impact of this posttranslational modification. These mutations reduce or even abolish barttin palmitoylation (Fig. 2). It appears possible that the substitution of cysteine by serine by itself changes the function of CLC-K/barttin channels. The following two reasons argue against this possibility. Serine and cysteine side chains are very similar, and it thus appears unlikely that their exchange affects the conformation of barttin and the CLC-K/barttin association. Accordingly, we did not observe alterations in single channel properties and voltage dependence of hClC-Ka co-expressed with single mutant barttin. Moreover, the chaperone function of barttin, promoting CLC-K channel insertion into the plasma membrane, remained unaffected. A comparison of the effects of the two single mutations and the double mutation on barttin palmitoylation and macroscopic current amplitudes demonstrates that these two values are proportional to each other (Fig. 3). This finding is in full agreement with the notion that the mutations decrease chloride currents by affecting barttin palmitoylation.

Impaired barttin palmitoylation leaves subcellular distribution of CLC-K and barttin unaltered (Fig. 5) but reduces macroscopic current amplitudes significantly (Fig. 3). These two results indicate that a smaller percentage of CLC-K/barttin channels is simultaneously active. At first glance this conclusion appears to be in disagreement with the results of noise

analysis which showed identical absolute open probabilities. However, noise analysis only provides information about channel opening and closing within time periods of the underlying experiments (Fig. 4). Taken together, biochemical and electrophysiological results indicate that a lack of palmitoylation causes long-lasting closed states or results in permanent closure of non-palmitoylated channels. Such a mechanism of channel regulation is not novel (43); however, there are much more examples of posttranslational modification of ion channels resulting in gradual modification of functional properties such as open probability or unitary current amplitude.

Tajima *et al.* (44) recently proposed barttin binding to the B- and J-helices of CLC-K. These two helices represent the longest transmembrane domains in CLC channels and are tilted by ~45° within the cell membrane (45). Binding of palmitate has been proposed to result in elongation of hydrophobic protein domains or even to tilt transmembrane helices (19, 46). Palmitoylation, therefore, might adjust the orientation of barttin within the lipid bilayer. It is tempting to speculate that association of barttin with these channel domains might result in altered orientation and thus change channel function.

The pronounced effect of barttin palmitoylation on CLC-K/barttin channel function suggests that this regulatory pathway might modify chloride conductances in the thin and thick ascending limb of the loop of Henle and permit adjusting urinary concentration and water excretion to variable fluid intake. However, we observed only minor changes in palmitoylation levels of barttin in mice upon water deprivation or upon increased water intake during a salt diet. For both conditions expression levels of barttin remained unchanged. Water deprivation in rats has been previously reported to result in between 1.7- and 4-fold up-regulation of rClC-K1, the homologue of human hClC-Ka (6, 47). This maneuver thus increases expression levels of CLC-K proteins to much higher levels than barttin palmitoylation. These findings suggest that palmitoylated barttin is excessively available in epithelial cells of Henle's loop so that even significant increases in the number of CLC-K channels will result in the formation of functional CLC-K/barttin channels.

We did not investigate barttin palmitoylation in distinct sections of the nephron separately. It thus appears possible that barttin palmitoylation is regulated in certain sections of the nephron by the water and salt intake. In contrast to up-regulation of rClC-K1 in the thin ascending limb of the Henle loop, the expression of rat rClC-K2, *i.e.* the homologue of human hClC-Kb, is not altered by dehydration (47). Because chloride conductance in the thick ascending limb of the Henle loop is exclusively mediated by ClC-K2/Kb, its regulation under water deprivation might be restricted to changes in barttin palmitoylation. Under conditions of sufficient water supply reduced palmitoylation of barttin may result in chloride accumulation in the cytoplasm of the thick ascending limb epithelial cells. This is expected to slow down the uptake of sodium chloride by the Na/K/2Cl transporter at the apical membrane and save energy by reducing the rate of the basolateral Na^+-K^+-ATPase.

In our experiments animals were exposed to water restriction for 1 day or salt diet for 1 week. These experiments thus only permitted identification of long term effects on palmitoylation levels. Dynamic palmitoylation events that take place within minutes or hours (48–50) might contribute to rapid adjustment and fine tuning of urinary concentration. The identification of palmitoyl-acyl transferases, which are involved in the posttranslational modification of barttin, might clarify the dynamics of the process and its potential for the adaptation of renal chloride currents.

Mutations in *BSND* cause Bartter syndrome type IV, a disorder of kidney function and hearing (1, 9, 28, 40, 41). The severity of renal symptoms varies widely between barttin mutations (28, 29, 40, 41). In recent years we have studied the functional consequences of several *BSND* mutations and found a clear correlation between changes in barttin function in heterologous expression systems and the severity of the clinical symptoms (4, 28, 29). We now tested three naturally occurring disease-associated mutations and observed distinct alterations in posttranslational modification of mutant barttin.

G47R results in sensorineural deafness in all patients and causes kidney disease of varying severity. Whereas initial reports describe a lack of characteristic renal symptoms as polyhydramnios, premature labor, or severe salt loss in neonatal period in patients carrying the G47R mutation (51–53), later work demonstrated that this mutation can also result in end-stage renal disease (54). In heterologous expression systems, G47R did not abolish activation of hClC-Kb/barttin channels but reduced macroscopic currents to ~10–15% as compared with WT barttin without affecting membrane insertion (28). We now demonstrate that palmitoylation of G47R barttin is decreased to a very similar extent (to 12.3 ± 3.0% ($n = 3$) of WT barttin). Taken together, these results suggest that G47R might exert its effects on barttin function at least partially via changes in palmitoylation. When heterologously expressed together with hClC-Ka or hClC-Kb in mammalian cells, R8W and G10S result in reduction of macroscopic current amplitudes by >90% (28). Our results now demonstrate that R8W reduce barttin palmitoylation to 44.6 ± 7.2% ($n = 3$), whereas G10S leaves this modification unaffected (Fig. 6). These mutations most likely cause chloride channel dysfunction independently of barttin palmitoylation, for example by conformational changes that impair the interaction with CLC-K channels.

In summary, here we demonstrate that barttin palmitoylation almost exclusively affects the function of CLC-K/barttin channels and thus may permit a rapid and reversible regulation of epithelial chloride conductance. Approaches that interfere with barttin palmitoylation might allow the development of novel diuretic agents for anti-hypertensive treatment.

Acknowledgments—We thank Dr. Brent R. Martin, University of Michigan, for discussing pharmacological tools to test the functional consequences of reduced barttin palmitoylation, Dr. Frank Schweda, Universität Regensburg, for support in designing experiments under high salt diet and providing us with animal food enriched with sodium chloride, Dr. Al George for providing the expression constructs for hClC-Ka, hClC-Kb, and barttin, Drs. Alexi Alekov and Gabriel Stölting for helpful discussions, and Toni Becher, Birgit Begemann, Ursula Jensen, and Petra Kilian for excellent technical assistance.

References

1. Estévez, R., Boettger, T., Stein, V., Birkenhäger, R., Otto, E., Hildebrandt, F., and Jentsch, T. J. (2001) Barttin is a Cl^- channel β-subunit crucial for renal Cl^- reabsorption and inner ear K^+ secretion. *Nature* **414,** 558–561
2. Uchida, S., and Sasaki, S. (2005) Function of chloride channels in the kidney. *Annu. Rev. Physiol* **67,** 759–778
3. Jentsch, T. J. (2008) CLC chloride channels and transporters: from genes to protein structure, pathology, and physiology. *Crit. Rev. Biochem. Mol. Biol.* **43,** 3–36
4. Fahlke, C., and Fischer, M. (2010) Physiology and pathophysiology of ClC-K/barttin channels. *Front Physiol.* **1,** 155
5. Kieferle, S., Fong, P., Bens, M., Vandewalle, A., and Jentsch, T. J. (1994) Two highly homologous members of the ClC chloride channel family in both rat and human kidney. *Proc. Natl. Acad. Sci. U.S.A.* **91,** 6943–6947
6. Matsumura, Y., Uchida, S., Kondo, Y., Miyazaki, H., Ko, S. B., Hayama, A., Morimoto, T., Liu, W., Arisawa, M., Sasaki, S., and Marumo, F. (1999) Overt nephrogenic diabetes insipidus in mice lacking the CLC-K1 chloride channel. *Nat. Genet.* **21,** 95–98
7. Simon, D. B., Bindra, R. S., Mansfield, T. A., Nelson-Williams, C., Mendonca, E., Stone, R., Schurman, S., Nayir, A., Alpay, H., Bakkaloglu, A., Rodriguez-Soriano, J., Morales, J. M., Sanjad, S. A., Taylor, C. M., Pilz, D., Brem, A., Trachtman, H., Griswold, W., Richard, G. A., John, E., and Lifton, R. P. (1997) Mutations in the chloride channel gene, *CLCNKB*, cause Bartter's syndrome type III. *Nat. Genet.* **17,** 171–178
8. Schlingmann, K. P., Konrad, M., Jeck, N., Waldegger, P., Reinalter, S. C., Holder, M., Seyberth, H. W., and Waldegger, S. (2004) Salt wasting and deafness resulting from mutations in two chloride channels. *N. Engl. J. Med.* **350,** 1314–1319
9. Birkenhäger, R., Otto, E., Schürmann, M. J., Vollmer, M., Ruf, E. M., Maier-Lutz, I., Beekmann, F., Fekete, A., Omran, H., Feldmann, D., Milford, D. V., Jeck, N., Konrad, M., Landau, D., Knoers, N. V., Antignac, C., Sudbrak, R., Kispert, A., and Hildebrandt, F. (2001) Mutation of *BSND* causes Bartter syndrome with sensorineural deafness and kidney failure. *Nat. Genet.* **29,** 310–314
10. Waldegger, S., Jeck, N., Barth, P., Peters, M., Vitzthum, H., Wolf, K., Kurtz, A., Konrad, M., and Seyberth, H. W. (2002) Barttin increases surface expression and changes current properties of ClC-K channels. *Pflugers Arch.* **444,** 411–418
11. Hayama, A., Rai, T., Sasaki, S., and Uchida, S. (2003) Molecular mechanisms of Bartter syndrome caused by mutations in the *BSND* gene. *Histochem. Cell Biol.* **119,** 485–493
12. Scholl, U., Hebeisen, S., Janssen, A. G., Müller-Newen, G., Alekov, A., and Fahlke, C. (2006) Barttin modulates trafficking and function of ClC-K channels. *Proc. Natl. Acad. Sci. U.S.A.* **103,** 11411–11416
13. Fischer, M., Janssen, A. G., and Fahlke, C. (2010) Barttin activates ClC-K channel function by modulating gating. *J. Am. Soc. Nephrol.* **21,** 1281–1289
14. Bosmans, F., Milescu, M., and Swartz, K. J. (2011) Palmitoylation influences the function and pharmacology of sodium channels. *Proc. Natl. Acad. Sci. U.S.A.* **108,** 20213–20218
15. Chien, A. J., Carr, K. M., Shirokov, R. E., Rios, E., and Hosey, M. M. (1996) Identification of palmitoylation sites within the L-type calcium channel β2a subunit and effects on channel function. *J. Biol. Chem.* **271,** 26465–26468
16. Qin, N., Platano, D., Olcese, R., Costantin, J. L., Stefani, E., and Birnbaumer, L. (1998) Unique regulatory properties of the type 2a Ca^{2+} channel β subunit caused by palmitoylation. *Proc. Natl. Acad. Sci. U.S.A.* **95,** 4690–4695
17. Shipston, M. J. (2011) Ion channel regulation by protein palmitoylation. *J. Biol. Chem.* **286,** 8709–8716
18. Tian, L., Jeffries, O., McClafferty, H., Molyvdas, A., Rowe, I. C., Saleem, F., Chen, L., Greaves, J., Chamberlain, L. H., Knaus, H. G., Ruth, P., and Shipston, M. J. (2008) Palmitoylation gates phosphorylation-dependent regulation of BK potassium channels. *Proc. Natl. Acad. Sci. U.S.A.* **105,** 21006–21011
19. Charollais, J., and Van Der Goot, F. G. (2009) Palmitoylation of membrane proteins (Review). *Mol. Membr. Biol.* **26,** 55–66
20. Hayashi, T., Rumbaugh, G., and Huganir, R. L. (2005) Differential regulation of AMPA receptor subunit trafficking by palmitoylation of two distinct sites. *Neuron* **47,** 709–723
21. Hayashi, T., Thomas, G. M., and Huganir, R. L. (2009) Dual palmitoylation of NR2 subunits regulates NMDA receptor trafficking. *Neuron* **64,** 213–226
22. Jeffries, O., Geiger, N., Rowe, I. C., Tian, L., McClafferty, H., Chen, L., Bi, D., Knaus, H. G., Ruth, P., and Shipston, M. J. (2010) Palmitoylation of the S0-S1 linker regulates cell surface expression of voltage- and calcium-activated potassium (BK) channels. *J. Biol. Chem.* **285,** 33307–33314
23. Allen, J. A., Halverson-Tamboli, R. A., and Rasenick, M. M. (2007) Lipid raft microdomains and neurotransmitter signalling. *Nat. Rev. Neurosci.* **8,** 128–140
24. Ho, G. P., Selvakumar, B., Mukai, J., Hester, L. D., Wang, Y., Gogos, J. A., and Snyder, S. H. (2011) *S*-Nitrosylation and *S*-palmitoylation reciprocally regulate synaptic targeting of PSD-95. *Neuron* **71,** 131–141
25. Ponimaskin, E. G., Heine, M., Joubert, L., Sebben, M., Bickmeyer, U., Richter, D. W., and Dumuis, A. (2002) The 5-hydroxytryptamine(4a) receptor is palmitoylated at two different sites, and acylation is critically involved in regulation of receptor constitutive activity. *J. Biol. Chem.* **277,** 2534–2546
26. Renner, U., Glebov, K., Lang, T., Papusheva, E., Balakrishnan, S., Keller, B., Richter, D. W., Jahn, R., and Ponimaskin, E. (2007) Localization of the mouse 5-hydroxytryptamine(1A) receptor in lipid microdomains depends on its palmitoylation and is involved in receptor-mediated signaling. *Mol. Pharmacol.* **72,** 502–513
27. Baekkeskov, S., and Kanaani, J. (2009) Palmitoylation cycles and regulation of protein function. *Mol. Membr. Biol.* **26,** 42–54
28. Janssen, A. G., Scholl, U., Domeyer, C., Nothmann, D., Leinenweber, A., and Fahlke, C. (2009) Disease-causing dysfunctions of barttin in Bartter syndrome type IV. *J. Am. Soc. Nephrol.* **20,** 145–153
29. Riazuddin, S., Anwar, S., Fischer, M., Ahmed, Z. M., Khan, S. Y., Janssen, A. G., Zafar, A. U., Scholl, U., Husnain, T., Belyantseva, I. A., Friedman, P. L., Riazuddin, S., Friedman, T. B., and Fahlke, C. (2009) Molecular basis of DFNB73: mutations of *BSND* can cause nonsyndromic deafness or Bartter syndrome. *Am. J. Hum. Genet.* **85,** 273–280
30. Imbrici, P., Liantonio, A., Gradogna, A., Pusch, M., and Camerino, D. C. (2014) Targeting kidney CLC-K channels: Pharmacological profile in a human cell line versus Xenopus oocytes. *Biochim. Biophys. Acta* **1838,** 2484–2491
31. Hebeisen, S., and Fahlke, C. (2005) Carboxy-terminal truncations modify the outer pore vestibule of muscle chloride channels. *Biophys. J.* **89,** 1710–1720
32. Wan, J., Roth, A. F., Bailey, A. O., and Davis, N. G. (2007) Palmitoylated proteins: purification and identification. *Nat. Protoc.* **2,** 1573–1584
33. Hautmann, M., Friis, U. G., Desch, M., Todorov, V., Castrop, H., Segerer, F., Otto, C., Schütz, G., and Schweda, F. (2007) Pituitary adenylate cyclase-activating polypeptide stimulates renin secretion via activation of PAC1 receptors. *J. Am. Soc. Nephrol.* **18,** 1150–1156
34. Sesti, F., and Goldstein, S. A. (1998) Single-channel characteristics of wild-type IKs channels and channels formed with two minK mutants that cause long QT syndrome. *J. Gen. Physiol.* **112,** 651–663
35. Sigworth, F. J. (1977) Sodium channels in nerve apparently have two conductance states. *Nature* **270,** 265–267
36. Alekov, A. K., and Fahlke, C. (2009) Channel-like slippage modes in the human anion/proton exchanger ClC-4. *J. Gen. Physiol.* **133,** 485–496
37. Nothmann, D., Leinenweber, A., Torres-Salazar, D., Kovermann, P., Hotzy, J., Gameiro, A., Grewer, C., and Fahlke, C. (2011) Hetero-oligomerization of neuronal glutamate transporters. *J. Biol. Chem.* **286,** 3935–3943
38. Tauber, R., Schenck, I., Josić, D., Gross, V., Heinrich, P. C., Gerok, W., and Reutter, W. (1986) Different oligosaccharide processing of the membrane-integrated and the secretory form of gp 80 in rat liver. *EMBO J.* **5,** 2109–2114
39. Hanwell, D., Ishikawa, T., Saleki, R., and Rotin, D. (2002) Trafficking and cell surface stability of the epithelial Na^+ channel expressed in epithelial Madin-Darby canine kidney cells. *J. Biol. Chem.* **277,** 9772–9779
40. Jeck, N., Reinalter, S. C., Henne, T., Marg, W., Mallmann, R., Pasel, K., Vollmer, M., Klaus, G., Leonhardt, A., Seyberth, H. W., and Konrad, M. (2001) Hypokalemic salt-losing tubulopathy with chronic renal failure and

sensorineural deafness. *Pediatrics* **108,** E5
41. Landau, D., Shalev, H., Ohaly, M., and Carmi, R. (1995) Infantile variant of Bartter syndrome and sensorineural deafness: a new autosomal recessive disorder. *Am. J. Med. Genet.* **59,** 454–459
42. Davda, D., El Azzouny, M. A., Tom, C. T., Hernandez, J. L., Majmudar, J. D., Kennedy, R. T., and Martin, B. R. (2013) Profiling targets of the irreversible palmitoylation inhibitor 2-bromopalmitate. *ACS Chem. Biol.* **8,** 1912–1917
43. Wolfe, J. T., Wang, H., Howard, J., Garrison, J. C., and Barrett, P. Q. (2003) T-type calcium channel regulation by specific G-protein $\beta\gamma$ subunits. *Nature* **424,** 209–213
44. Tajima, M., Hayama, A., Rai, T., Sasaki, S., and Uchida, S. (2007) Barttin binds to the outer lateral surface of the ClC-K2 chloride channel. *Biochem. Biophys. Res. Commun.* **362,** 858–864
45. Dutzler, R., Campbell, E. B., Cadene, M., Chait, B. T., and MacKinnon, R. (2002) X-ray structure of a ClC chloride channel at 3.0 Å reveals the molecular basis of anion selectivity. *Nature* **415,** 287–294
46. Kandasamy, S. K., and Larson, R. G. (2006) Molecular dynamics simulations of model trans-membrane peptides in lipid bilayers: a systematic investigation of hydrophobic mismatch. *Biophys. J.* **90,** 2326–2343
47. Vandewalle, A., Cluzeaud, F., Bens, M., Kieferle, S., Steinmeyer, K., and Jentsch, T. J. (1997) Localization and induction by dehydration of ClC-K chloride channels in the rat kidney. *Am. J. Physiol.* **272,** F678–F688
48. Chamberlain, L. H., Lemonidis, K., Sanchez-Perez, M., Werno, M. W., Gorleku, O. A., and Greaves, J. (2013) Palmitoylation and the trafficking of peripheral membrane proteins. *Biochem. Soc. Trans.* **41,** 62–66
49. Kang, R., Wan, J., Arstikaitis, P., Takahashi, H., Huang, K., Bailey, A. O., Thompson, J. X., Roth, A. F., Drisdel, R. C., Mastro, R., Green, W. N., Yates, J. R., 3rd, Davis, N. G., and El-Husseini, A. (2008) Neural palmitoyl-proteomics reveals dynamic synaptic palmitoylation. *Nature* **456,** 904–909
50. Rocks, O., Gerauer, M., Vartak, N., Koch, S., Huang, Z. P., Pechlivanis, M., Kuhlmann, J., Brunsveld, L., Chandra, A., Ellinger, B., Waldmann, H., and Bastiaens, P. I. (2010) The palmitoylation machinery is a spatially organizing system for peripheral membrane proteins. *Cell* **141,** 458–471
51. Brum, S., Rueff, J., Santos, J. R., and Calado, J. (2007) Unusual adult-onset manifestation of an attenuated Bartter's syndrome type IV renal phenotype caused by a mutation in *BSND*. *Nephrol. Dial. Transplant.* **22,** 288–289
52. García-Nieto, V., Flores, C., Luis-Yanes, M. I., Gallego, E., Villar, J., and Claverie-Martín, F. (2006) Mutation G47R in the *BSND* gene causes Bartter syndrome with deafness in two Spanish families. *Pediatr. Nephrol.* **21,** 643–648
53. Miyamura, N., Matsumoto, K., Taguchi, T., Tokunaga, H., Nishikawa, T., Nishida, K., Toyonaga, T., Sakakida, M., and Araki, E. (2003) Atypical Bartter syndrome with sensorineural deafness with G47R mutation of the β-subunit for ClC-Ka and ClC-Kb chloride channels, barttin. *J. Clin. Endocrinol. Metab.* **88,** 781–786
54. Park, C. W., Lim, J. H., Youn, D. Y., Chung, S., Lim, M. H., Kim, Y. K., Chang, Y. S., and Lee, J. H. (2011) Renal dysfunction and barttin expression in Bartter syndrome Type IV associated with a G47R mutation in *BSND* in a family. *Clin. Nephrol.* **75,** 69–74